

Dependence on the deposition conditions in the adsorption of C_6H_8 molecules on a Si(100)- 2×1 surface

F. D'Amico,¹ R. Gunnella,¹ M. Shimomura,² T. Abukawa,³ and S. Kono³

¹CNISM—Università di Camerino, Via Madonna delle Carceri, 62032 Camerino, Macerata, Italy

²Research Institute of Electronics, Shizuoka University, Hamamatsu 432-8011, Japan

³Institute of Multidisciplinary Research for Advanced Materials, Tohoku University, Sendai 980-8577, Japan

(Received 28 March 2007; revised manuscript received 24 June 2007; published 23 October 2007)

We studied the molecular 1,4-cyclohexadiene (CHD) adsorption at room temperature on a Si(100)- 2×1 surface, from the first stages up to saturation [about half a monolayer (ML)] at two different deposition rates. The chemical configuration of the adsorbed CHD on the silicon surface was obtained by valence band and C 1s core level photoemission analyses. Such a molecular adsorption, at the earlier stages and low rates, showed only weak features of chemical bonding with Si; at higher coverages ($\theta > 0.3$ ML) and higher deposition rates, a chemisorption occurred with an upright structure of the molecule, in which one out of the two unsaturated π orbitals reacted to form a bond with the silicon dimer. The whole investigation is based on an accurate determination of the strongly asymmetric C 1s core level components obtained by means of an angular resolved photoelectron diffraction analysis.

DOI: [10.1103/PhysRevB.76.165315](https://doi.org/10.1103/PhysRevB.76.165315)

PACS number(s): 68.43.Fg, 79.60.Dp

I. INTRODUCTION

Adsorption of organic molecules on a Si(100)- 2×1 surface has been recently studied to incorporate the functionalization on a semiconducting surface.¹ Organic molecules are also widely used as buffer layers to grow chemisorbed molecular organic films² of very recent interest for moletronics applications. Another motivation is the use of hydrocarbons as precursors for chemical vapor deposition of silicon carbide and diamond film growth.³⁻⁵ In all these investigations, particularly intriguing is the role of the interface between the organic film and the substrate.

One class of interesting system to study is represented by the unsaturated organic molecules on Si surfaces. Unsaturated organic molecules can react with one Si dimer (di- σ bonding) through a [2+2]-type cycloaddition,⁶ in which one C=C double bond is saturated; alternately, two opposite C=C double bonds can be saturated by two adjacent Si dimers (dual [2+2]).⁷ The former reaction leads to an upright structure, while the result of the latter reaction is a more planar configuration. Reactions known as [4+2] or “Diels-Alder” cycloadditions can also be obtained by interaction with one Si dimer to form a six-membered ring of carbon atoms⁶ as in the case of benzene adsorption on Si(100).⁸

The demand of experimental investigations of adsorbed hydrocarbon systems is far from being unjustified as theoretical predictions in local density approximation are often challenged by (1) localization and/or delocalization of the cyclic molecules interacting on the solid surface, (2) the huge unit cell volume, and (3) the van der Waals forces characterizing such systems.

Quite recently, great interest was drawn by the adsorption of 1,4-cyclohexadiene (CHD) on a Si(100)- 2×1 surface. Theoretical studies⁹⁻¹¹ were performed to assess the structure of such a system. From the total energy point of view, the favored structure is pedestal-like, in which both the π bonds are saturated by two adjacent silicon dimers (dual [2+2]). Nevertheless, no hint of bridge or pedestal adsorption is

found by experiments using techniques such as ultraviolet photoelectron spectroscopy (UPS), low energy electron diffraction (LEED),¹² high-resolution electron energy loss spectroscopy,^{13,14} and scanning tunneling microscopy.^{15,16} While all these methods confirmed quite qualitatively an upright structure of the molecule, a more quantitative confirmation of this structure has been obtained by x-ray photoelectron diffraction (PD).^{17,18} Immediately before the submission of this paper, we acquired knowledge of the work of Kato *et al.*¹⁹ They observed the coexistence of both upright and pedestal configurations on a Si(100)- 2×1 surface when CHD is chemisorbed at room temperature (RT) and at low coverages, while a weakly bound π -complex state was discovered at lower temperatures (85 K).

Considering the above scenario, it can be argued that the dependence of the adsorption mechanism on the deposition rate and coverage is likely playing an important but still unclear role. In fact, as specifically described for the present system by Cho *et al.*,¹⁰ the effects of the kinetic barriers to reaction paths on the surface should be taken into account for an accurate description of the adsorption process.

We present below a different experimental investigation by means of photoelectron spectroscopies from both core (C 1s) and valence band (VB) states of the RT behavior of 1,4-CHD deposited at two different rates on a Si(100)- 2×1 surface. For the core level analysis, we took advantage of a previous PD¹⁸ experiment for the part concerning the cumbersome decomposition and assignment of the atomic origin of each component of the spectrum.

The work is organized as follows: Sec. II reports an experimental description of the several stages of the sample preparation. Section III reports the study of the VB spectra of CHD molecules adsorbed on the Si(100). Section IV is a brief discussion about the correct deconvolution procedure necessary to obtain a reliable fit in the C 1s core level spectra. In Sec. V are reported the results of the C 1s asymmetric peak fits obtained following the indications of Sec. IV. The VB and the C 1s fit results are finally compared and discussed in Sec. VI. Conclusions will follow in Sec. VII.

II. EXPERIMENTAL DETAILS

Synchrotron radiation photoelectron spectroscopy measurements were performed at the beamline BC-13C at KEK-PF facility in Japan and at the VUV beamline at Elettra, Italy. VB and carbon $1s$ core level photoelectrons were collected by using photons with energies of 50 and 330 eV, respectively. The electric field was linearly polarized in the plane containing the photon beam and the detection direction. A Si(100) substrate was flashed at 1250 °C and annealed at 1000 °C until a sharp 2×1 reconstruction was obtained at LEED. After that, sufficient time (1–2 h) was necessary for the sample to cool down to RT. Then, the surface was exposed to the CHD gas (purity better than 99%), purified by freeze-pump-thaw cycles before the exposure.

In the first experiment, a quasi-single-domain 2×1 -Si(100) surface (80% domain ratio) was prepared to increase the angular anisotropy and the signal-to-noise ratio of the PD experimental data.¹⁸ In such an experiment, a high dosing rate was provided by a pulse valve connected to a tube for an efficient delivery of the gas to the sample. The PD experiment on the quasi-single-domain consisted of a large data set with almost 400 spectra taken at high resolution along different θ angles (between 30° and 80° from the normal to the surface) and ϕ angles (between 0° and 120° from the dimer bond direction [110]). The vacuum during the gas dosing was kept in the 10^{-10} Torr range to minimize molecule decomposition by pumps or gauges. A mass spectrometer was used for gas partial pressure measurements during the deposition. The 2×1 LEED spots were observed even after saturation of CHD adsorption, suggesting that the dimers on the silicon surface and the domain ratio were preserved.

In a second experiment on a double-domain surface, the gas was dosed through a leak valve, which precisely controlled the gas inlet. We deposited CHD in two steps: (1) in the first stage at low rate (8×10^{-5} L/s), up to a coverage of 0.3 ML; and (2) in the second stage, by increasing the deposition rate up to 8×10^{-4} L/s and to a coverage of about 0.5 ML, close to saturation conditions (1 ML is defined as one molecule adsorption per Si dimer). After that, the sample was heated resistively at a temperature of 200 °C; in doing so we obtained the same chemisorbed phase of the first experiment on a single domain.¹⁸ The temperature was measured by means of an optical pyrometer for $T > 250$ °C, while below such a limit, an extrapolation from the pyrometer data as a function of the sample current was used. In the final stage, the sample was heated to 400 °C for 10 min.

VB and core level photoemissions reported below are related mainly to the double-domain experiment at different coverages and deposition rates.

III. VALENCE BAND RESULTS

Here, we present the UPS results for the relevant surfaces obtained during the experiment, namely, (i) the clean Si(100)- 2×1 double-domain surface, (ii) the surface after adsorption of 0.3 ML of 1,4-CHD at a low deposition rate, and (iii) the surface after a total coverage of 0.4 ML at high

deposition rate, obtained as a result of short (10 min) annealing at 200 °C. It is important to stress that in the latter case (iii), the same conditions can be achieved either directly, by a high rate deposition, or, starting from surface (ii), by deposition at a high rate and annealing at 200 °C for 10 min.

Figure 1 shows from (a) to (d) the VB spectra taken with electron emission normal to the surface (NE) (photoelectron polar angle $\theta=0^\circ$), and from (e) to (g), the normal photon incidence (NI) spectra at $\theta=45^\circ$. All the spectra are taken along the [110] direction on the surface (photoelectron azimuth angle $\phi=0^\circ$) corresponding, because of the double-domain surface, either to a Si dimer bond or to a dimer row direction. Only curve (b) is taken along the [100] direction ($\phi=45^\circ$). Spectra (a) and (e) are taken on the clean 2×1 -Si(100) surface, where the peak A, at a binding energy (BE) of 0.8 eV, corresponds to the silicon dimer states.^{20,21} Such a state is seen to persist up to spectra (b)–(c) and (f), which are taken after depositing 0.3 ML of CHD. Finally, spectra (d) and (g) are obtained after depositing CHD for a total amount of 0.4 ML at a higher deposition rate and annealing at 200 °C. In normal emission from (a) to (d), both the in-plane and out-of-plane components of the electric field along the [110] direction are present; in (b) the in-plane component is directed along [100]. Spectra from (e) to (g) have only in-plane components of the electric field oriented along the [110] direction.

A visual inspection of Fig. 1 puts in evidence the presence of two electronic states at 2.3 and 4.0 eV, which can be related to the highest occupied molecular orbitals of the unsaturated CHD [Figs. 1(a)–1(c) and 1(f)], and are partially saturated at the increase of the coverage and subsequent annealing. As a consequence, a single unsaturated state is observed at 3.8 eV in Fig. 1(g) as reported in literature.¹² All these observations point toward the existence of a previously unnoticed weakly bonded absorption state of CHD on silicon before the onset of chemisorption.

IV. C 1s CORE LEVEL DECONVOLUTION

The line shape analysis of the C $1s$ core level (at the photon energy of 330 eV) has been performed considering the asymmetry on the high BE side of the core levels as a signature of the inelastic effects. Such effects must be carefully included to avoid unjustified higher BE core level components. We follow the work of Yamashita *et al.*²² to describe the high asymmetry of the photoemission core levels within the Frank-Condon scheme as due to vertical transitions between the initial core electron ground state to the electronically and vibrationally excited state. In the linear coupling approximation, an asymmetric component is obtained by a linear composition of Voigt functions (Gaussian line shape convoluted to a Lorentzian function), equally spaced ($\hbar\omega$) and whose intensities are $I_n = e^{-S} S^n / n!$ for $n=0, 1$, and 2. The S factor is defined as $\delta^2 \mu \omega / 2 \hbar$, where δ , μ , and ω , are respectively the normal coordinate of the core excitation, the reduced mass, and the vibrational frequency.²² In the case of ethylene on Si, the latter frequency has been demonstrated, by the isotope effect, to be close to the value of the C—H stretching vibration.²²

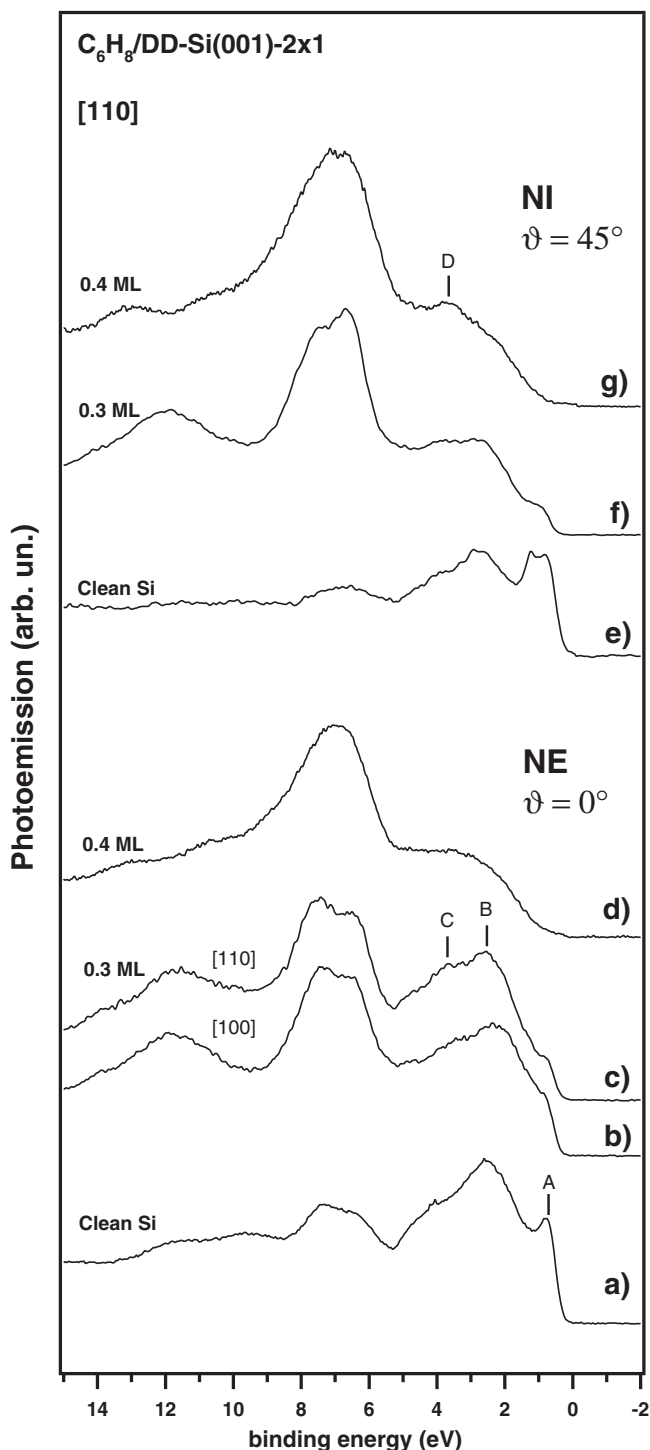


FIG. 1. Valence Band spectra taken on the $C_6H_8/2 \times 1$ -Si(100) surface in NE from (a) to (d), and in NI from (e) to (g). In (a) and (e) are reported the spectra of the clean Si(100)- 2×1 surface; (b), (c), and (f) report the spectra of weakly bound adsorption on the silicon surface (0.30 ML); and (d) and (g) report the spectra of C_6H_8 chemisorbed on silicon with a coverage of 0.4 ML after annealing at 200 °C. The electric field, due to the double domain, is equally directed along the dimer rows [1-10] and the dimer bond direction [110]. In (b), the component of the electric field in the plane is directed along the [100] direction. The photoelectron direction has an angle θ of 45° with respect to the surface normal.

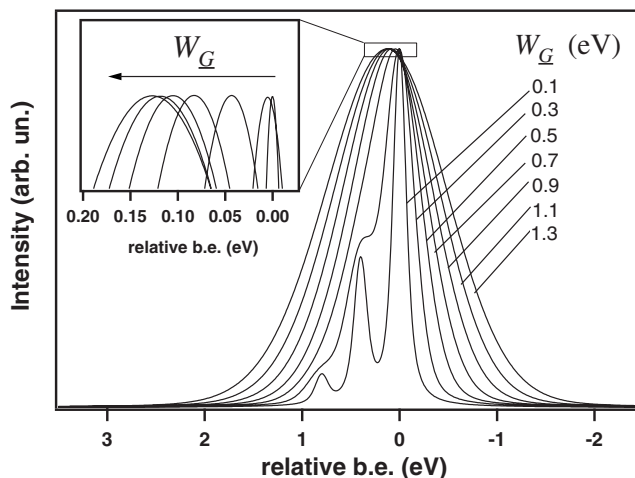


FIG. 2. Plots of a single asymmetric component simulated using three Voigt functions according to the model of Ref. 22. A fixed Lorentzian FWHM (W_L) at 0.1 eV is used, while the Gaussian FWHM (W_G) is varied from 0.2 to 1.3 eV. The inset reports the shift observed in the peak maximum position.

In order to reduce the arbitrariness in the decomposition of the core levels, we aim at estimating the importance of the asymmetric components in the core level peak for the values of the signal-to-noise ratio and the energy resolution of the present experiment.

For simplicity, we simulated in Fig. 2 only one chemical component under the realistic hypothesis that the C—H stretching vibration has an energy of 400 meV and the S parameter has a value of 0.4,^{18,22} then, for each Frank-Condon component, we plotted the spectrum obtained considering one Voigt line shape, i.e., the convolution of a Gaussian and a Lorentzian component.

In a photoemission spectrum, the Lorentzian width is related to the mean lifetime of the core hole and represents a physical characteristic of the system, while the Gaussian width is related to the thermal broadening and the experimental resolution from both monochromator and electron analyzer. In the hypothesis of an S parameter equal to 0.4 (Ref. 22) for every chemical shift component, we approximate the linear combination with the first three terms, i.e., by three Voigt line shapes of intensity I_n separated from each other by 400 meV.

For the chosen values of S and $\hbar\omega$, we have plotted in Fig. 2 the curves obtained for a Lorentzian full width at half maximum (FWHM) W_L of 100 meV and a Gaussian FWHM W_G varying between 0.1 and 1.3 eV. The zero of the relative BE is fixed at the maximum of the elastic photoemission peak. In Fig. 2, we can observe how, by increasing the W_G , it is no longer possible to resolve the three peaks while the curves become strongly asymmetric. Increasing again the W_G , the curve shape loses the asymmetry and becomes similar to a Gaussian line shape. Another important effect that can be observed is the shift of the curve maximum to a higher value of BE (see the inset in Fig. 2). This shift amounts to 0.15 eV for a W_G of 1.3 eV and must be taken into account if a symmetric Voigt function is used for the chemical shift component.

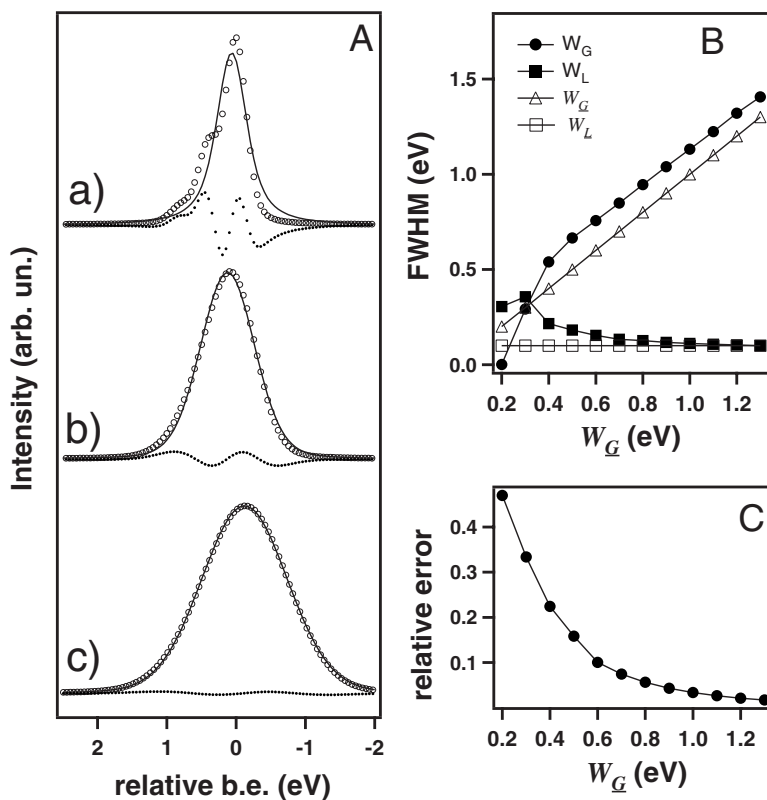


FIG. 3. (A) Results of the fits of the three Voigt simulated components (circles) using one Voigt function (solid line). (B) Values of W_G and W_L FWHM (solid symbols) obtained by fitting the line shapes of Fig. 2 with a single Voigt function. For comparison, the nominal values of W_G used in Fig. 2 are reported as empty symbols. (C) Relative error of the approximation of the fitting of the three Voigt simulated components using one Voigt function at different values of the resolution (W_G).

It would be useful to know in which range the three-peak curves of Fig. 2 could be approximated correctly by a single component Voigt function with three free parameters: the amplitude, the Gaussian FWHM (W_G), and the Lorentzian FWHM (W_L). We underline that W_G and W_L are the parameters for the symmetric Voigt line shape, while only W_G and W_L have physical meaning related to the component of the asymmetric core level. Figure 3(a) reports three curves at different values of W_G equal to 0.3, 0.7, and 1.3 eV [curves (a), (b), and (c), respectively].

It can be shown how by increasing the W_G , i.e., reducing the experimental energy resolution, the difference between the two models is reduced and a single component Voigt line shape accurately fits the chemical shift component. On the other hand, if the experimental noise is important, we can make use of the symmetric Voigt line shape to fit the experimental data. More quantitatively, Fig. 3(c) reports the relative error of the approximation (residual) normalized to the peak maximum as a function of the W_G . We can conclude that a simple rule of thumb is that the experimental curve might be approximated by a symmetric Voigt function in all the cases in which the experimental noise at the given experimental resolution is above the curve in Fig. 3(c).

Furthermore, we establish how the W_G and W_L are related to the parameters of the three Voigt line shapes (W_G and W_L). In Fig. 3(b) are reported the values of the W_G and W_L obtained by the fit. For comparison the W_G and W_L of the

curves plotted in Fig. 2 are also reported on the y axis. By this comparison, we observe that W_G is always larger than W_G ; this is due to the superposition of three Voigt line shapes, leading to a wider peak, i.e., at low resolution energy spectra, the W_G obtained by fitting is overestimated. On the contrary, we can observe that the W_L of the Voigt fit reaches the same value of the W_L at low energy resolution. The discrepancy at high energy resolution is due to the bad quality of the fit, as we can see from the fit (a) of Fig. 3(a).

Now we have all the elements to establish if our experimental data must be fitted correctly with three Voigt components or if it is possible to use simply one Voigt line shape per component. For simplicity, the chemical shift components obtained by a fit with three Voigt line shapes, related to the parameters W_G , W_L , S , and $\hbar\omega$, will be called “asymmetric” components, while the chemical shift components obtained by a fit with one Voigt line shape with parameters W_G and W_L will be called “symmetric” components.

The present experiment corresponds to a point below the plot of Fig. 3(c) where the experimental relative error is 2% and the overall resolution is 0.25 eV. As a consequence, the C 1s photoemission peaks must be mandatorily fitted with asymmetric components. In Figs. 4(b) and 4(c), we report the fit of a core level taken at $\theta=45^\circ$ and $\phi=0^\circ$ using three asymmetric and symmetric components, respectively. While the quality of the fit is comparable [Fig. 4(a)], the results we obtain in the case of an asymmetric or a symmetric line shape deconvolution are quite different as reported in Figs.

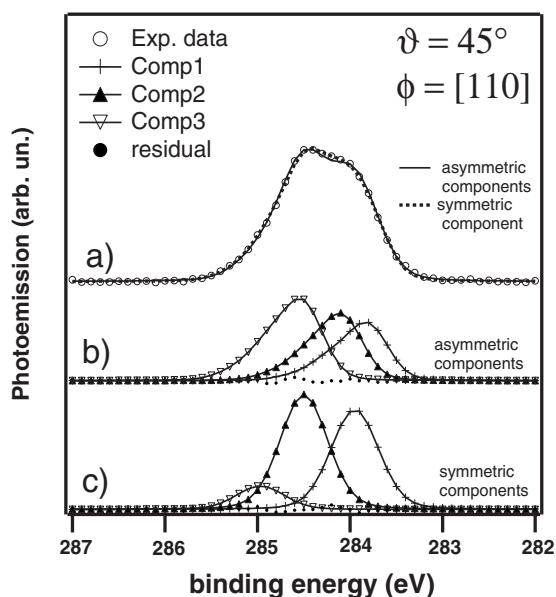


FIG. 4. C 1s core level shift decomposition obtained with asymmetric and symmetric chemical shift components, respectively. From top to bottom, we find (a) total signal, (b) decomposition with asymmetric line shapes, and (c) decomposition with symmetric line shapes.

4(b) and 4(c), respectively. We observe that the main consequence of using symmetric line shapes is the appearance of a third minor component at high BE [see Fig. 4(c)]. Such a component is necessary to fit the high BE tail of the spectra. On the contrary, using three asymmetric chemical shift line shapes, we obtain components with comparable intensities [Fig. 4(b)] as expected considering the number of the non-equivalent C atoms of the molecule.

The deconvolution procedure might take advantage of the structural analysis performed by means of multiple scattering calculations²³ of the core level angular anisotropy.¹⁸ In fact, the PD anisotropy, defined by normalizing the photoemission intensities (I) for each θ polar angle of collection as $(I - I_{min}) / (I_{max} - I_{min})$, must point to the same atomic structure for each resolved chemical shift component. This is a strong constraint to be fulfilled, and makes the core level component analysis reliable and the interpretation free of faults.

Figure 5 shows, from top to bottom, the C 1s photoelectron diffraction intensities¹⁸ resolved into components at the binding energy reported in the figure after a standard residual minimization procedure, obtained with three asymmetric line shapes (left panel) and three symmetric line shapes (right panel). The fits are based on more than 1000 core level spectra. The plot showed how the angular anisotropies obtained in Fig. 5 using the two procedures were different, leading to inconsistent results for the structural problem.

V. C 1s CORE LEVEL RESULTS

With the aim of understanding the problem of the adsorption by means of C 1s core level photoemission, in Fig. 6, we report the spectra taken along the [110] direction with the

photoelectron making an angle of 45° with respect to the normal to the surface. All the spectra are normalized to the core level component at 284.0 eV BE.

At a coverage of 0.3 ML, deposited at slow rate [Fig. 6(b)], only two C 1s components separated by 0.42 eV are obtained by the fit analysis with asymmetric line shapes. On this basis, we can assert that in this first stage, the molecule does not experience any bonding with the Si surface. After the saturation (0.50 ML), a third component at lower kinetic energy (-0.28 eV) appears [Fig. 6(c)]. However, only after annealing at 200°C as in Fig. 6(d) is the surface identical to the one obtained, by a higher deposition rate and reported in Fig. 6(a), on the quasi-single-domain surface. In Fig. 6(d), the appearance of a small bump at 283.2 eV BE is due to defect formation and C dissolution inside the silicon.²⁴ This effect is accompanied by a similar appearance of a minor defect component in the Si 2p core levels (not shown) at 101 eV BE.

Finally, Fig. 6(e) reports the C 1s fit after the annealing at 400°C . A clear modification of the core level is observed, probably due to the dehydrogenation with a consequent strong reduction of the C—C single bond component in the C 1s core level. From the peak area, the dissolution of carbon inside the Si is estimated to be about 20%.

VI. DISCUSSION

In order to interpret the valence band measurements, a direct comparison with multilayers of physisorbed CHD molecules makes us conclude that the two states corresponding respectively to the orbitals $\pi C=C^-$ and $\pi C=C^+$ (Ref. 12) are still present in the very first stage of our experiment.

Such occupied states have an even symmetry with respect to the plane perpendicular to the double C bond. To detect this state, the electric field should lie perpendicular to the nodal plane of the π states, i.e., perpendicular to the molecular plane. In the case of a planar adsorption of an intact molecule, it would be possible to detect orbital states in NE by means of the electric field component perpendicular to the molecular plane. In fact, a sizable intensity in Figs. 1(b) and 1(c) of peaks labeled B and C (at the energies of 2.3 and 4.0 eV, respectively) is observed with respect to the normal incidence case reported in Fig. 1(f). Furthermore, curves in Figs. 1(b) and 1(c), taken along two nonequivalent directions, look very similar, indicating a minor anisotropy on the surface.

If the molecule were chemisorbed upright, the electric field should be either parallel or perpendicular to the dimer rows as in the experimental geometry of Fig. 1(g), corresponding to a coverage of 0.4 ML after annealing at 200°C . Such a spectrum shows, at variance with the previous case, a single state (D) at 3.8 eV due to one out of two unsaturated π states which does not react on the Si(100)- 2×1 surface. Correctly enough, such a state is strongly suppressed in the case of the spectrum in Fig. 1(d) (NE), where the electric field is not completely perpendicular to the molecular plane.

It is worth noting that VB spectra resembling those of Figs. 1(b) and 1(c) were measured in the case of benzene butterfly-like adsorption on Si(100).^{8,25} Such spectra, show-

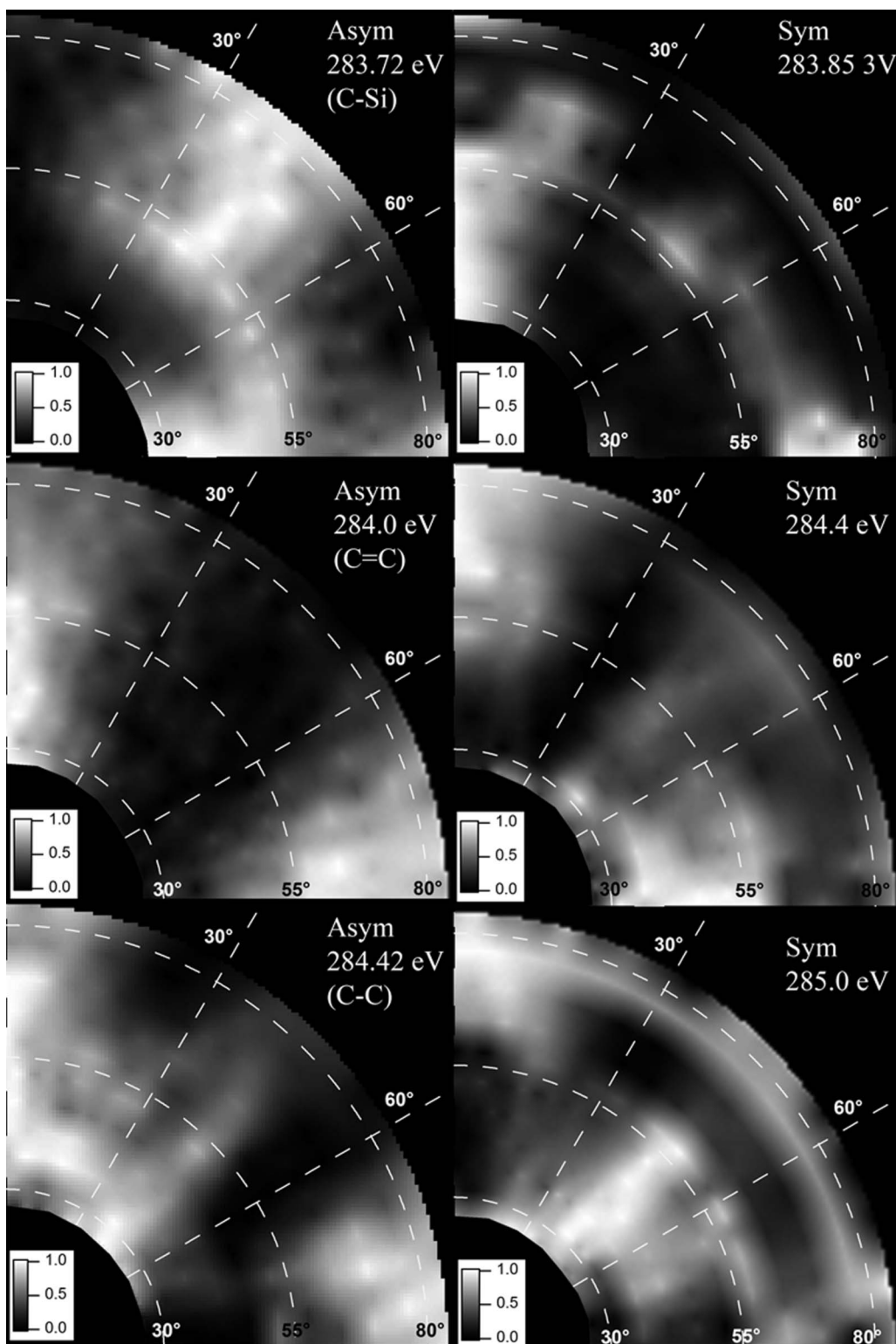


FIG. 5. PD anisotropies of the C 1s core level decomposition of 0.4 ML of 1,4-CHD on quasi-single-domain Si(100)- 2×1 surface. The panel on the left makes use of asymmetric component analysis, while the panel on the right makes use of symmetric components. The direction $\phi=0$ corresponds to the minority dimer bond direction.

ing the conservation of the double π unsaturated orbitals (valence states at 2.3 and 4.0 eV, respectively), could be a hint of possible dehydrogenation effects of the CHD molecule before adsorption. Nevertheless, the latter explanation

can be excluded on the basis of the C 1s core level analysis which will follow.

From the point of view of C 1s core level measurements consistent conclusions with VB results can be achieved. We

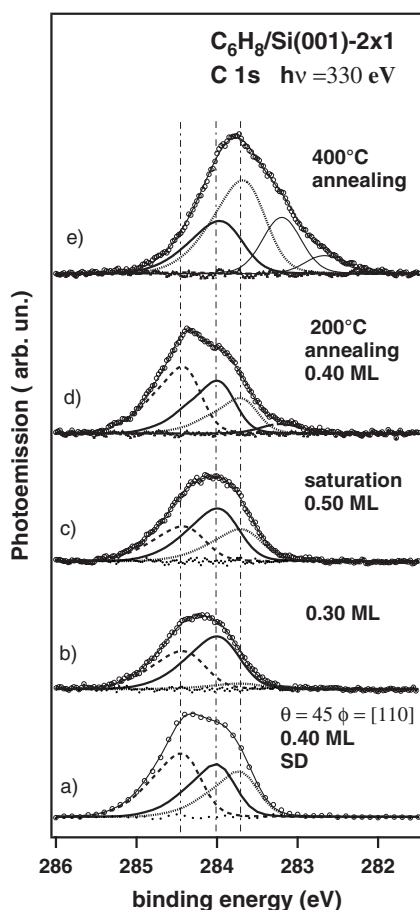


FIG. 6. C 1s core level of 1,4-CHD at different experimental stages. In (a) is reported the C 1s peak fit obtained in Ref. 18 on a single-domain 2×1 -Si(100) surface close to saturation and decomposed according to three asymmetric core levels. In (b) is reported the fit obtained with 0.30 ML after a low rate deposition, (c) reports the fit at surface saturation, (d) and (e) report the fit obtained after annealing at 200 and 400 °C, respectively.

follow the study of Oltedal *et al.*²⁶ about the C 1s core level spectrum of the gas phase 1,4-CHD. In this work, the spectrum is considered made by a cyclohexanelike (C_6H_{12}) component due to single bond C—C carbon atoms, and one less bound component (0.48 eV) due to the four C=C double bond carbon atoms. In the case of adsorption on Si, a third component is expected due to the bonding with Si dimers as evidenced by the VB signature [D in Fig. 1(g)] of the unsaturated π state at the coverage of 0.4 ML following the annealing at 200 °C.

Such a result is confirmed by the C 1s core level analysis of spectra reported in Fig. 6(d) on the basis of a proper assignment of core level peaks of the surface formed on the single domain surface [Fig. 6(a)].¹⁸

For these two latter spectra [Figs. 6(a) and 6(d)], the C 1s core level analysis can be summarized in Table I. Two chemical shifts with respect to the C=C component located at 284.0 eV were considered; the chemical state of Si—C σ bond at lower energy (−0.28 eV) and the C—C single bond at 0.42 eV higher BE, respectively. In Table I are also re-

TABLE I. Line shape parameters for the deconvolution of the C 1s core level taken from Ref. 18.

Component	C—C	C=C	C—Si
Binding energy (eV)	284.42	284.0	283.72
S	0.48	0.42	0.40
$\hbar\omega$ (eV)	0.37	0.37	0.40

ported the optimized parameters used to describe the asymmetric core levels.

A very different scenario is observed before the onset of the upright chemisorption [Fig. 6(b)]. In such a case, deconvolution results exclude the presence of the Si—C formation in the spectrum of Fig. 6(b) after 0.3 ML deposition. Any attempt to obtain three chemical shift components (upright chemisorption) or two components with an energy separation of 0.70 eV between Si—C and C—C single bond components (pedestal chemisorption) was unsuccessful. Analogously, the possible configuration suggested by VB measurements, with two unsaturated orbitals at 2.3 and 4.0 eV, closely resembling benzene adsorption on Si(001) at low coverages^{8,25} with C_σ (Si—C single bond) and C_π (C=C double bond) components in the 2:1 ratio, can be ruled out. In fact, a larger C 1s chemical shift (0.42 eV), compared with that of 0.30 eV found by Kim *et al.*,⁸ has been measured. Moreover, considering the evolution of the spectra [Figs. 6(c) and 6(d)], a clear-cut assignment of the σ Si—C bond at a binding energy of 283.7 eV is made, while only a negligible contribution of this component is found in Fig. 6(b).

Summarizing, while no apparent differences have been recorded in the photoemission core levels at the two experimental stages when a pulse valve supplying a high deposition rate was used either at low coverages (0.2–0.3 ML) or at saturation (0.5 ML), the findings observed by Kato *et al.*¹⁹ on the first stages of absorption of CHD/Si(001)- 2×1 surface are somewhat confirmed using a slow deposition rate. In the present work, we comply with the remarkable difference that even at RT a clear signature of the Si—C bonding is lacking in the presence of low deposition rates at low coverages; such a character has been singled out by means of a core level shift photoemission analysis. This is particularly rather puzzling because chemisorption with a pedestal geometry, predicted by the total energy calculation and observed by Kato *et al.*,¹⁹ should be easily achieved in the case of a long time scale¹⁰ of the experiment. Nonetheless, the hypothesis that a pedestal molecule bonded to two Si dimers could show a major change in the values of the core level shifts, somewhat upsetting the present adopted scheme, should not be completely neglected, but should be taken into proper experimental and theoretical considerations to elucidate still unclear aspects of the kinetics of the CHD-on-Si system.

VII. CONCLUSIONS

We have studied the 1,4-CHD adsorption at different deposition rates and at RT. The analysis has shown a

weakly bound adsorption at a rate of 8×10^{-5} L/s and a chemisorption at 8×10^{-4} L/s or higher. Such an analysis is based on valence band photoemission, showing at a low deposition rate the presence of unsaturated C $2p$ orbital states.

Moreover, it is shown how, by means of a suitable model of peak analysis with proper attention to asymmetric tails, C $1s$ core level photoemission can provide information which is remarkably complementary to the information obtainable with valence band photoemission.

-
- ¹A. Filler and S. F. Bent, *Prog. Surf. Sci.* **73**, 1 (2003).
²R. A. Wolkow, *Annu. Rev. Phys. Chem.* **101**, 9581 (1997).
³G. P. Lopinski, D. J. Moffatt, D. D. M. Wayner, and R. A. Wolkow, *Nature (London)* **392**, 909 (1998).
⁴M. De Crescenzi, R. Bernardini, S. Pollano, R. Gunnella, P. Castrucci, G. Dufour, and F. Rochet, *Surf. Sci.* **489**, 185 (2001).
⁵T. Takaoka, H. Saito, Y. Igari, and I. Kusunoki, *J. Cryst. Growth* **183**, 175 (1998).
⁶R. Konecny and D. Doren, *Surf. Sci.* **417**, 169 (1998).
⁷F. Rochet, F. Bournel, J. J. Gallet, G. Dufour, L. Lozzi, and F. Sirotti, *J. Phys. Chem. B* **106**, 4967 (2002).
⁸Y. K. Kim, M. H. Lee, and H. W. Yeom, *Phys. Rev. B* **71**, 115311 (2005).
⁹K. Akagi and S. Tsuneyuki, *Surf. Sci.* **131**, 493 (1999).
¹⁰J. H. Cho, D. H. Oh, K. S. Kim, and L. Kleinman, *J. Chem. Phys.* **116**, 3800 (2002).
¹¹K. Akagi, S. Tsuneyuki, Y. Yamashita, K. Hamaguchi, and J. Yoshinobu, *Appl. Surf. Sci.* **234**, 162 (2004).
¹²K. Hamaguchi, S. Machida, K. Mukai, Y. Yamashita, and J. Yoshinobu, *Phys. Rev. B* **62**, 7576 (2000).
¹³M. Wakatsuchi, H. S. Kato, H. Fujisawa, and M. Kawai, *J. Electron Spectrosc. Relat. Phenom.* **137**, 217 (2004).
¹⁴F. Tao, Z. H. Wang, and G. Q. Xu, *Surf. Sci.* **530**, 203 (2003).
¹⁵K. Hamaguchi, S. Machida, M. Nagao, F. Yasui, K. Mukai, Y. Yamashita, J. Yoshinobu, H. S. Kato, H. Okuyama, M. Kawai, T. Sato, and M. Iwatsuki, *J. Phys. Chem. B* **105**, 3718 (2001).
¹⁶K. Hamaguchi, K. Mukai, Y. Yamashita, J. Yoshinobu, T. Sato, and M. Iwatsuki, *Surf. Sci.* **531**, 199 (2003).
¹⁷R. Gunnella, M. Shimomura, M. Munakata, T. Takano, T. Yamazaki, T. Abukawa, and S. Kono, *Surf. Sci.* **566**, 618 (2004).
¹⁸R. Gunnella, M. Shimomura, F. D'Amico, T. Abukawa, and S. Kono, *Phys. Rev. B* **73**, 235435 (2006).
¹⁹H. S. Kato, M. Wakatsuchi, M. Kawai, and J. Yoshinobu, *J. Phys. Chem. C* **111**, 2557 (2007).
²⁰F. J. Himpsel and D. E. Eastman, *J. Vac. Sci. Technol.* **16**, 1297 (1979).
²¹A. Goldmann, P. Kobe, W. Monch, G. Wolfgarten, and J. Pollmann, *Surf. Sci.* **169**, 438 (1986).
²²Y. Yamashita, S. Machida, M. Nagao, S. Yamamoto, K. Mukai, and J. Yoshinobu, *Chem. Phys. Lett.* **374**, 476 (2003).
²³R. Gunnella, F. Solal, D. Sebilliau, and C. R. Natoli, *Comput. Phys. Commun.* **132**, 251 (2000).
²⁴S. Contarini, S. P. Howlett, C. Rizzo, and B. A. De Angelis, *Appl. Surf. Sci.* **51**, 177 (1991).
²⁵S. Gokhale, P. Trischberger, D. Menzel, W. Widdra, H. Droge, H. P. Steinruck, U. Birkenheuer, U. Gutdeutsch, and N. Rosch, *J. Chem. Phys.* **108**, 5554 (1998).
²⁶V. M. Oltedal, K. J. Børve, L. J. Sæthre, T. D. Thomas, J. D. Bozek, and E. Kukk, *Phys. Chem. Chem. Phys.* **6**, 4254 (2004).